ISSN 1028-334X, Doklady Earth Sciences, 2024, Vol. 515, Part 2, pp. 652–657. © Pleiades Publishing, Ltd., 2024.
ISSN 1028-334X, Doklady Earth Sciences, 2024. © Pleiades Publishing, Ltd., 2024.

MINERALOGY

A New Atypical Case of Ferromanganese Mineralization in the Sea of Japan

O. N. Kolesnik[a,*], A. A. Karabtsov[b], V. T. S''edin[a], A. N. Kolesnik[a], and E. P. Terekhov[a]

Presented by Academician G.I. Dolgikh October 25, 2023

Received October 26, 2023; revised December 13, 2023; accepted December 14, 2023

Abstract—The first case of hydrothermal brecciated crusts composed of goethite with quartz veinlets is described for the Sea of Japan.

Keywords: goethite, quartz, hydrothermal vents, brecciation, North Yamato Ridge, Sea of Japan

DOI: 10.1134/S1028334X23603668

Expansion of demand for metals is a global trend. The reserves of terrestrial ore deposits are irreversibly depleting. As a consequence, interest in the study of ferromanganese formations (FMFs) of the oceans and seas is growing. In addition to iron and manganese, they contain copper, nickel, cobalt, gold, tellurium, molybdenum, bismuth, platinum, tungsten, zirconium, niobium, and rare earth elements [1].

Among Russian seas, the Sea of Japan is characterized by a wide distribution of FMFs. In the absolute majority of cases, FMFs of the Sea of Japan are hydrothermal, hydrothermal–sedimentary manganese crusts [2]. They are predominantly black in color, layered, and found in the apical parts of volcanic edifices located in deep-water basins (the most productive depth interval is 1500–2500 m). The main ore minerals of these FMFs are todorokite and birnessite. Recently, a series of scientific publications have described pyrolusite, goethite, and manganite crusts unusual for the Sea of Japan [3–5], as well as manganese conglomerates and breccias [6, 7]. Each new atypical case requires special consideration.

FMFs (15 fragments of ore crusts 2.5 to 3 cm thick) from the southern end of the North Yamato Ridge were the material used for the present study (Fig. 1). These ore crusts differ markedly from the usual FMFs of the Sea of Japan in the color, density, and structure.

[a]*V.I. Il'ichev Pacific Oceanological Institute, Far Eastern Branch, Russian Academy of Sciences, Vladivostok, 690041 Russia*
[b]*Far East Geological Institute, Far Eastern Branch, Russian Academy of Sciences, Vladivostok, 690022 Russia*
**e-mail: kolesnik_o@poi.dvo.ru*

The North Yamato Ridge is part of the undersea Yamato Upland, the largest in the Sea of Japan. The upland is characterized by a subcontinental type of crust. The geological structure of the upland includes rocks of different ages (from the Proterozoic to the Quaternary) and origin (igneous, metamorphic, sedimentary) [8–12]. In the relief of the southern end of the North Yamato Ridge (Fig. 1), there is a local rise, bounded on three sides by scarps 300–600 m high (horst?). The basement rocks in the study area are represented by Lower Cretaceous sandstones, silty-sandstones, and siltstones (thickness of the sequence is at least 300 m) and by presumably Upper Paleozoic granitoids. The Cenozoic sedimentary cover is absent or of insignificant thickness. Samples of ore crusts were dredged on the indicated local rise within the southern, steepest scarp (station 1410, dredging interval is 1000–1100 m, 28th voyage of R/V Pervenets, 1978) (Fig. 1). The Lower Cretaceous quartz sandstones, medium- and fine-grained, massive, with slip mirrors, were taken together with the crusts.

The ore crusts were studied in the laboratories of the Il'ichev Pacific Oceanological Institute, Far Eastern Branch, Russian Academy of Sciences, and in the Center for Common Use, Far Eastern Geological Institute, Far East Branch, Russian Academy of Sciences, according to the established scheme. The research included visual inspection and light microscopy (structure), hydrostatic weighing (density), X-ray powder diffraction analysis (mineral composition), and electron microprobe analysis (microstructure, chemical composition) [3–6].

According to the results, the ore crusts from station 1410 have similar physical properties, structure, and material composition.

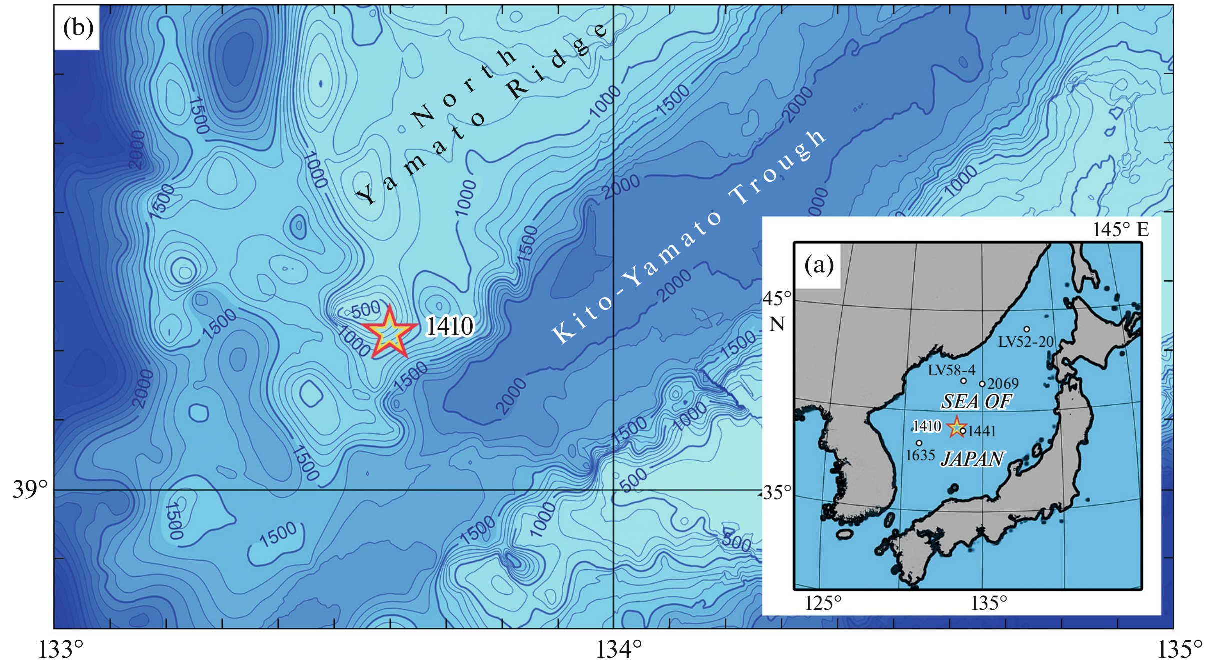

Fig. 1. Map of the study area. (a) Position of the dredging station of the factual material (asterisk) and the stations where FMFs atypical for the Sea of Japan were found earlier (dots): LV58-4, pyrolusite crusts [3]; 1635, goethite crusts [4]; 1441, manganite crusts [5]; LV52-20, manganese conglomerates [6]; and 2069, manganese breccias [7]. (b) Relief with the dredging station of the factual material (asterisk). Isobaths, m (GEBCO, 2022).

The density of the ore crusts from station 1410 averages 3.04 g/cm^3, whereas the density of ordinary todorokite–birnessite FMFs of the Sea of Japan is not more than 2 g/cm^3 [3]. The obtained values are comparable to the density of goethite (3.03 g/cm^3) and pyrolusite (3.35 g/cm^3) crusts, which are rare for the Sea of Japan [3, 4].

The ore crusts from station 1410 are characterized by a brown color unusual for FMFs of the Sea of Japan and consist almost entirely of goethite (Figs. 2, 3; Table 1). This is the second finding of goethite crusts in the Sea of Japan. They were first detected as single samples at station 1635 (Fig. 1). The thickness of the crusts from station 1635 did not exceed 2 cm; goethite was represented by two varieties—yellow loose (in main mass) and black dense with luster from matte to brilliant (in interlayers) [4]. Saw cuts of the crusts from station 1410 show that they are dense, massive, with brilliant luster (type 1 zones), with traces of brecciation (type 2 zones), and with abundant quartz veinlets (Fig. 2). The association of goethite with veinlet quartz was revealed in the ore crusts of the Sea of Japan for the first time.

Breccia crusts of todorokite–birnessite composition, common for the FMFs of the Sea of Japan, were encountered earlier only at station 2069 [7]. In the uppermost part of the ore crusts from station 1410, a layer with a thickness of no more than 0.3 cm is distinguished; it consists of yellow loose goethite without quartz veinlets. Comparison of X-ray diffraction patterns of the matter of different goethite crusts of the Sea of Japan showed almost complete identity of the position of goethite reflexes with some difference in intensity, which is probably due to the presence or absence of quartz crusts in the material. Quartz reflexes sometimes overlap reflexes of goethite (Fig. 3, Table 1). This conclusion is confirmed by the results of previous studies, according to which limonite/goethite varieties have no principal X-ray differences [13]. The upper surface of the crusts from station 1410 is smoothed, with a thin black film (todorokite) on some fields. On the upper and lateral surfaces, there are insignificantly developed loose excretions of whitish yellow, whitish green color (illite). The lower surface is rough, with traces of detachment, which may indicate that it belongs to the main, larger ore crust (occurrences?).

In the chemical composition of the ore crusts from station 1410, iron and oxygen (up to 37 wt % for each of the elements) dominated dramatically; they contain a significant amount of silica (up to 16 wt %) and a small admixture of other elements (Table 2). The comparison of the composition of zones of types 1–3 in the light of their textural–structural and mineralogical characteristics (Figs. 2–4) have shown that the zones of type 1 are relatively enriched in silica and oxygen due to the presence of quartz veins in goethite. The total sum of elements here is maximum due to the

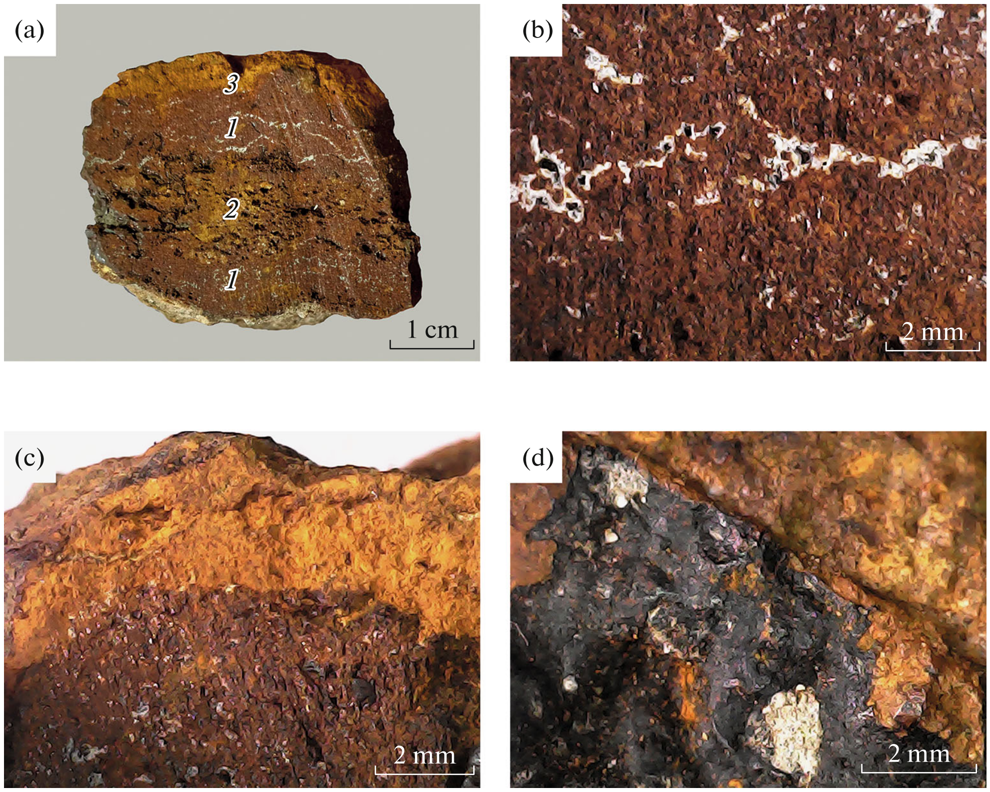

Fig. 2. General view, structure, and mineral composition of the ore crusts from station 1410 on the basis of visual inspection, microscope examination, and X-ray powder diffraction analysis. (a) Surface of a saw cut with the numbers of distinguished zones: (*1*) brown goethite, dense variety; (*2*) brown goethite, brecciation zone; (*3*) yellow goethite, loose variety. (b) White veinlets of quartz in dense brown goethite of a zone of type 1. (c) Boundary between brown goethite of a zone of type 1 and yellow goethite of a zone of type 3. (d) Black film of todorokite with local whitish illite on yellow goethite of the zone of type 3.

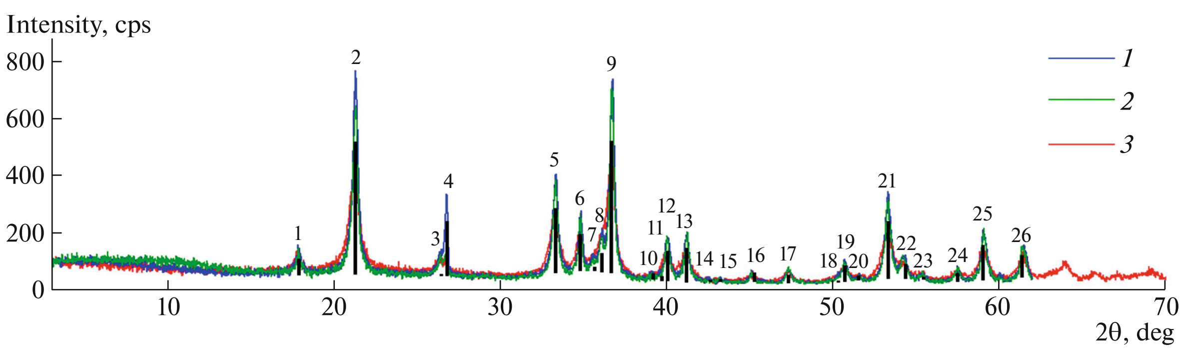

Fig. 3. X-ray diffraction patterns of the matter of goethite crusts of the Sea of Japan (Cu *K*α-radiation, monochromator on the secondary beam): (*1*, *2*) goethite crust from station 1410, brown matter of a zone of type 1 and yellow matter of a zone of type 3, respectively (Fig. 3a); (*3*) goethite crust 1635/7-3, black interlayer [4]. Interpretation of reflexes 1–26 for the crust from station 1410, zone of type 1 (Table 1).

dense, massive structure of the material. The zones of type 2, respectively, are enriched in sodium, potassium, and aluminum, because goethite, in addition to quartz veinlets, contains small fragments of nonmetallic minerals of an irregular, angular shape, often intersected by goethite veinlets (brecciation zones). The total sum of elements here is lower due to the porosity of the matter. The content of potassium, chlorine, and sulfur increases slightly in the transition from zones of type 1 to zones of type 3. The total content of elements here is minimal due to the loose texture of the matter.

Earlier analysis of the distribution of ferromanganese, phosphorite, and barite ore occurrences in the Sea of Japan showed their attribution to the tectoni-

Table 1. Table of reflexes to the X-ray diffraction pattern of ore crust material from station 1410, zone of type 1 (Figs. 2a, 3)

Reflex no.	2θ, deg	*D*-space, Å	Relative intensity *I*, %	Mineral phase	Standard card number, 00-ICDD
1	17.89	4.95	11.77	Goethite	00-029-0713
2	21.29	4.17	100.00	Goethite, quartz	00-029-0713, 01-070-7344
3	26.45	3.37	0.66	Goethite	00-029-0713
4	26.79	3.33	40.92	Quartz	01-070-7344
5	33.33	2.69	48.00	Goethite	00-029-0713
6	34.83	2.57	27.55	Goethite	00-029-0713
7	35.69	2.51	2.66	Goethite	00-029-0713
8	36.13	2.484	14.03	Goethite	00-029-0713
9	36.69	2.447	99.21	Goethite, quartz	00-029-0713, 01-070-7344
10	39.19	2.297	4.81	Goethite	00-029-0713
11	39.71	2.268	2.93	Quartz	01-070-7344
12	40.06	2.249	22.52	Goethite	00-029-0713
13	41.19	2.190	25.44	Goethite	00-029-0713
14	42.64	2.119	1.55	Quartz	01-070-7344
15	43.26	2.090	2.41	Goethite	00-029-0713
16	45.30	2.000	6.45	Goethite	00-029-0713
17	47.35	1.918	6.48	Goethite	00-029-0713
18	50.37	1.810	0.60	Quartz	01-070-7344
19	50.72	1.799	12.07	Goethite, quartz	00-029-0713, 01-070-7344
20	51.57	1.771	3.31	Goethite	00-029-0713
21	53.34	1.716	42.56	Goethite	00-029-0713
22	54.36	1.686	10.74	Goethite	00-029-0713
23	55.48	1.655	2.03	Goethite, quartz	00-029-0713, 01-070-7344
24	57.51	1.601	5.79	Goethite, quartz	00-029-0713, 01-070-7344
25	59.03	1.564	26.60	Goethite	00-029-0713
26	61.40	1.509	16.67	Goethite	00-029-0713

Table 2. Chemical composition of the ore crust from station 1410 based on the results of electron microprobe analysis, wt %

Element	Zone of type 1 *				Zone of type 2 *				Boundary of zones of types 1 and 3 *			
	measured	σ	norm.	σ	measured	σ	norm.	σ	measured	σ	norm.	σ
O	37.90	0.59	41.11	0.35	33.74	0.60	39.56	0.44	22.28	0.47	36.62	1.33
Na	–	1.34	0.11	1.57	0.12	0.23	0.10	0.38	0.15			
Mg	0.25	0.09	0.27	0.10	0.35	0.08	0.41	0.10	0.36	0.05	0.59	0.07
Al	–	3.03	0.09	3.55	0.12	0.36	0.02	0.59	0.05			
Si	16.14	0.10	17.51	0.15	9.24	0.10	10.83	0.10	4.20	0.13	6.89	0.09
P	0.45	0.05	0.48	0.05	0.39	0.03	0.46	0.03	0.40	0.06	0.66	0.10
S	–	–	0.13	0.03	0.21	0.06						
Cl	–	0.06	0.02	0.07	0.03	0.26	0.03	0.43	0.04			
K	–	0.46	0.03	0.54	0.03	0.06	0.02	0.10	0.04			
Ca	0.12	0.03	0.13	0.03	0.21	0.02	0.25	0.03	0.46	0.03	0.75	0.03
Fe	37.34	0.17	40.50	0.26	36.44	0.14	42.74	0.35	32.14	1.54	52.77	1.25
Total	92.19		100.00		85.27		100.00		60.88		100.00	

* The analyzed areas are shown in Figs. 4a, 4d, and 4j, respectively. The dash designates that an element was not detected.

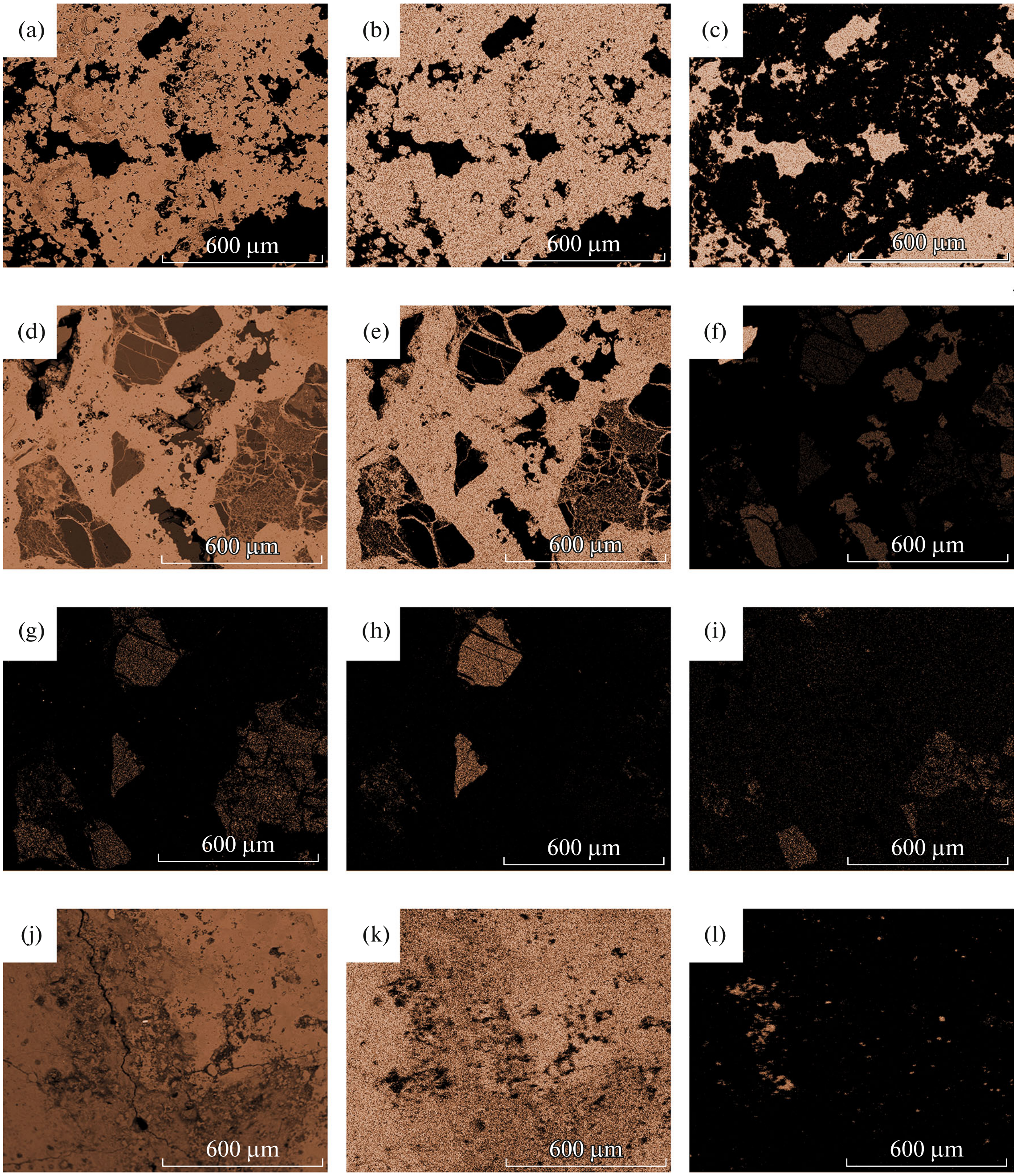

Fig. 4. The distribution pattern of chemical elements in the ore crust from station 1410 in a "false" brown color according to the results of electron microprobe analysis (crust structure with the zones distinguished in it (Fig. 2 a)). (a–c) Zone of type 1: (a) backscattered-electron image of the analyzed area, (b) Fe$K\alpha_1$, (c) Si$K\alpha_1$. (d–i) Zone of type 2: (d) backscattered-electron image of the analyzed area, (e) Fe$K\alpha_1$, (f) Si$K\alpha_1$, (g) Al$K\alpha_1$, (h) K$K\alpha_1$, (i) Na$K\alpha_1$, 2. (j–l) Boundary of zones of type 1 and type 3: (j) backscattered-electron image of the analyzed area, (k) Fe$K\alpha_1$, (l) Si$K\alpha_1$.

cally active areas of the sea bottom and their connection with hydrothermal processes [2]. This conclusion fully refers to the research area and the studied ore crusts on the basis of a number of facts:

(1) the rise, where the crusts are dredged, has a horst-like shape;

(2) rock fragments with slip mirrors are present in the dredged materials;

(3) the crusts have a brecciated, veinlet-like texture [14];

(4) crusts are markedly enriched in iron (goethite) and are depleted in manganese, the manganese content is below the analytical capabilities of a microprobe (in the hydrothermal process, iron and manganese are fractionated with deposition of pure iron or pure manganese matter; goethite or todorokite usually predom-

inate in hydrothermal FMFs of the near-spreading oceanic regions [15]);

(5) the crusts are markedly depleted in aluminum and titanium; the content of these elements in unbrecciated zones is below the analytical capabilities of a microprobe (aluminum and titanium are almost inert in the hydrothermal process; their content in hydrothermal FMFs does not exceed 0.3 and 0.1%, respectively [15]).

The identification of new cases of ferromanganese mineralization atypical for the Sea of Japan expands the range of regional variations in the FMF material composition and the conditions ore genesis.

FUNDING

This study was supported by the Russian Science Foundation, project no. 23-27-00004, https://rscf.ru/project/23-27-00004/.

CONFLICT OF INTEREST

The authors of this work declare that they have no conflicts of interest.

REFERENCES

1. Vestn. Ross. Akad. Nauk **89** (5), 513–514 (2019).
2. N. V. Astakhova, Russ. Geol. Geofiz. **62** (9), 977–986 (2021).
3. N. V. Astakhova, V. T. S"edin, A. V. Mozherovsky, and E. A. Lopatnikov, Dokl. Earth Sci. **462** (1), 453–458 (2015).
4. O. N. Kolesnik, A. A. Karabtsov, V. T. S"edin, and A. N. Kolesnik, Dokl. Earth Sci. **505** (2), 543–549 (2022).
5. O. N. Kolesnik, A. A. Karabtsov, V. T. S"edin, A. N. Kolesnik, and E. P. Terekhov, Dokl. Earth Sci. **511** (2), 672–678 (2023).
6. N. V. Astakhova, E. A. Lopatnikov, and I. B. Tsoy, J. Volcanol. Seismol. **9** (6), 358–368 (2015).
7. P. E. Mikhailik, E. V. Mikhailik, N. V. Zarubina, N. N. Barinov, V. T. S"edin, and E. P. Lelikov, Russ. J. Pac. Geol. **8** (5), 315–330 (2014).
8. I. I. Bersenev, E. P. Lelikov, V. L. Bezverkhnii, N. G. Vashchenkova, V. T. S"edin, E. P. Terekhov, and I. B. Tsoy, *The Sea of Japan: Bottom Geology* (Far Eastern Scientific Center of the USSR Acad. Sci., Vladivostok, 1987) [in Russian].
9. E. P. Lelikov and A. A. Pugachev, Petrology **24** (2), 196–213 (2016).
10. I. B. Tsoy, N. G. Vashchenkova, L. N. Vasilenko, M. T. Gorovaya, N. K. Vagina, and Yu. I. Mel'nichenko, Stratigr. Geol. Correl. **28** (2), 202–229 (2020).
11. E. P. Terekhov, T. A. Kharchenko, and N. S. Lee, Russ. J. Pac. Geol. **16** (2), 101–115 (2022).
12. E. P. Terekhov, V. S. Markevich, I. B. Tsoy, and N. N. Barinov, Russ. J. Pac. Geol. **17** (2), 147–164 (2023).
13. A. G. Betekhtin, *Mineralogy Course* (KDU, Moscow, 2007) [in Russian].
14. M. P. Isaenko, *Ores Textures and Structures: Guidebook,* 3rd ed. (Nedra, Moscow, 1983) [in Russian].
15. *Manganese and Ferromanganese Mineralization in Different Environmental Conditions: Investigations by Scanning Electron Microscopy,* Ed. by G. N. Baturin (Eslan, Moscow, 2012) [in Russian].

Translated by V. Krutikova